Determining the Position of Patroclus for the *Lucy* Mission Rendezvous

A. Baldacchino, Lab Partner: L. Thomson
L3 Astrolab, Epiphany Term
Submitted: 25th April 2018

The aim of our investigation was to study the Trojan asteroid Patroclus to determine its position for the 2033 flyby of the *Lucy* mission. Determining positions accurately is important to space agencies so they can perform orbital manoeuvres successfully and minimise the fuel required for their missions. Observations of a sample of 10 asteroids were taken over the course of 7 weeks, recording their Right-Ascensions and Declinations. This data was used in conjunction with archival data to increase the accuracy of the determined orbital parameters. The mean fractional uncertainty in the orbital parameters for Patroclus was improved from 8.1×10^{-4} to 3.5×10^{-7} with the inclusion of archival data. This increase in accuracy reduced the confidence volume of the error ellipsoid for Patroclus' position by a factor of $\sim 10^{11}$. This result is significant as high accuracy is required when performing orbital manoeuvres in order to achieve a flyby with a low relative distance between the spacecraft and the target object.

I. INTRODUCTION

Jupiter's Trojan asteroids are made up of two groups of asteroids, the Greek camp and the Trojan camp, which are positioned at Jupiter's L4 and L5 Lagrange points respectively. At the time of writing, there are $\sim$7,000 asteroids currently classified as Trojans with an asymetry in their distributions: the L4 point has $\sim$4,600 asteroids and the L5 point has $\sim$2,400.[1] Studying these asteroids is important to understanding the evolution of the early solar system; they can act as physical indicators of the conditions of the nebula in which they formed.

There is discussion in the literature as to how Jupiter's Trojans formed. Theories have varied and included being captured early in Jupiter's growth,[2] by collisions,[3] and due to the effects of gas drag.[4] Emery et al, (2015) discuss gas drag and capture during Jupiter's formation in more detail.[5] However, none of these methods can account for the broad $\sim 40°$ range in inclinations of their orbits that are observed and has warranted further theories to be explored.

Morbidelli et al, (2005) performed simulations exploring how the asteroids could have been captured immediately after Jupiter and Saturn crossed the 1:2 mean motion resonance (MMR).[6] Their results match the orbital distribution of the observed Trojan asteroids and can account for the large distributions in inclinations.

Nesvorný et al, (2013) build on the theory proposed by Morbidelli et al, (2005) developing their 'Jumping Jupiter' model. Instead of a smooth migration over the 2:1 MMR, it was instead thought that it 'jumped' from 2 to 2.3 when Jupiter and Saturn scattered off Uranus, Neptune or another body of similar mass.[7] This model also matches the orbital distributions of the observed Trojans and they propose that it could account for the asymmetry in the L4-L5 distributions with an ice giant passing near the the L5 point and depleting it of its bodies.

Due to the uncertain nature of the Trojan asteroids, and the lack of direct measurement by man-made satellites NASA approved the *Lucy* mission, which is planned to launch in October 2021. The aim of this mission is to investigate six of Jupiter's Trojans with its final flyby being of Patroclus in Jupiter's Trojan camp in March 2033.

Patroclus was selected as a worthwhile object to explore as it is one of the largest in its class of objects and is also in a binary system with its moon Menoetius, which is highly uncommon.[8] Observations of Patroclus can be used to calculate the orbital parameters of this binary system and can derrive low densities suggesting that Patroclus could con-

tain a large amount of water ice. This leads to the conclusion it was likely formed in the outer parts of the solar system.[9][10] The *Lucy* mission will perform observations using infrared spectrometers and high-resolution imaging devices that will resolve these outstanding questions.

For this mission to be able to proceed, the orbits of the bodies it plans to visit must be well defined. This allows an efficient flight plan to be constructed that minimises the amount of fuel required, and hence the total cost of the mission. It is also important that the tolerances in the orbital parameters measured are well known. As there is an error in the predicted position for asteroids at any given time, the mission is required to include some reserve fuel so that the spacecraft would still be able to reach its targets at the limits of their known tolerances.

The orbits of bodies can be determined through observations. If the body is observed on at least three different occasions and its Right Ascension (RA) and Declination (Dec) are measured, its orbital parameters can be determined. A body's orbital parameters completely define its Keplerian orbit and traditionally those six elements are: eccentricity (e), semi-major axis (a), inclination (i), longitude of the ascending node (Ω), argument of periapsis (ω) and true anomaly (ν). The parameters are represented in Fig. 1.

In this investigation the mean anomaly, M, is used in place of the true anomaly, ν. The true anomaly is defined as the angle between the periapsis-focus vector to the object-focus vector in the orbital plane. The mean anomaly is defined as the angle in the orbital plane between the periapsis-focus vector and the imaginary object-focus vector where the object is projected onto a circular orbit around the same body with the same orbital period where an equal area is swept out in a specific time. The main difference between these parameters is that M increases linearly in time whereas ν does not necessarily behave in the same way if the objects orbit is elliptical. The difference in these parameters is demonstrated in Fig. 2.

As minor body's are easily influenced by the larger bodies in the solar system, it is not correct to assume that their orbits are Keplerian. When a minor bodies orbital parameters are calculated, they should also be quoted with an epoch of osculation, the date and time these parameters were calculated. This is so that the Keplerian orbit can be perturbed to take account of gravity from other bodies in the solar system, radiation pressure, atmospheric drag and other effects. This results in the body's orbital path not being identical for each rotation which is in contradiction to the classical Keplerian orbit.
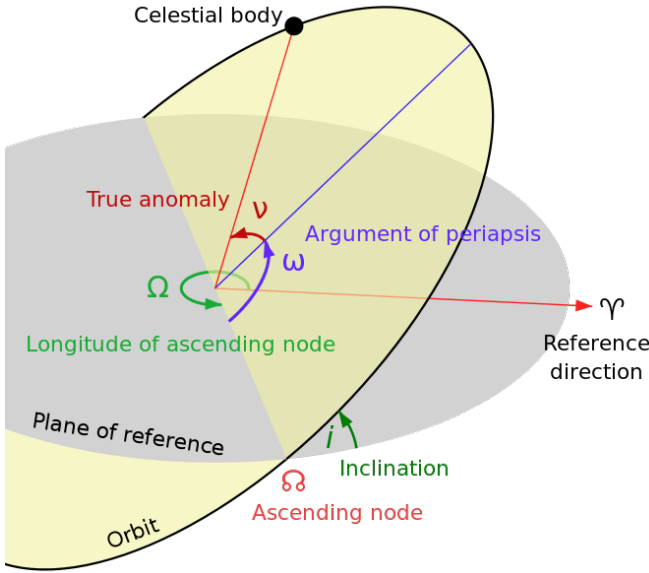
FIG. 1: A diagram of the orbital parameters typically used to define the orbit of a celestial body in the heliocentric frame. The longitude of ascending node (Ω), true anomaly (ν), argument of periapsis (ω) and inclination (i) are shown.[11]
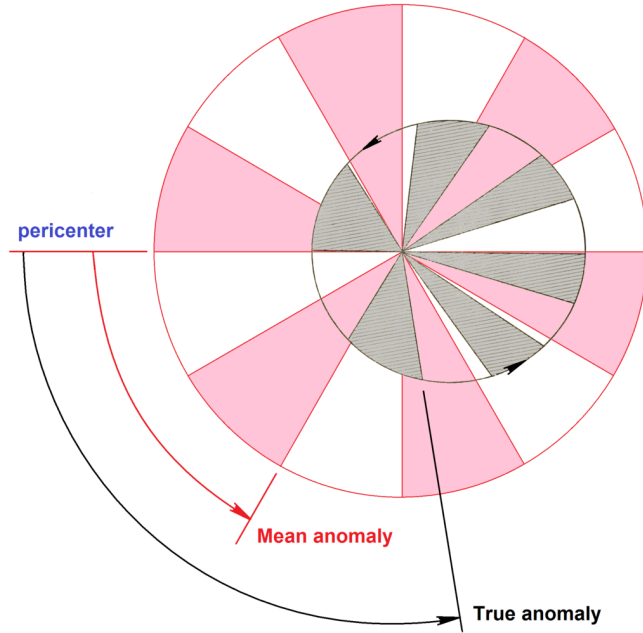

FIG. 2: A diagram comparing the mean anomaly and true anomaly orbital parameters in the plane of the orbit. The true anomaly corresponds to the angle on the ellipse at which the body is at. The mean anomaly corresponds to the position on the circle at which the body would be located, mean anomaly increases linearly with time.[12]

In this investigation we calculate the orbits of several Trojan asteroids, including the asteroid Patroclus, using clear band observations of the bodies. We find the accuracy to which we can measure these orbits in order to determine the tolerances on the position of the asteroid Patroclus when *Lucy* plans to rendezvous with it in March 2033.

II. METHOD

Initially a sample of asteroids that would be visible to us using our available equipment and time frame, our sample being further restricted to the Trojan camp of Jovian asteroids as this was the only group that was visible to us. The asteroids that we chose were: 1974 FV1, Anchises, Ilioneus, Memnon, Mentor, Pandarus, Paris, Patroclus, Priamus and Troilus. These asteroids were chosen because their greater height in the sky at observation times would allow for greater seeing; their greater apparent magnitudes would allow for greater signal to noise ratios; these asteroids had been observed previously which would allow us to use archival data, this is important when refining our results later in our investigation.

Observations were made on 10 different nights from the 25th January 2018 to the 10th March 2018 using a combination of the DRACO2, Far-East 16 and Pt5m telescopes. DRACO2 uses a 14-inch Meade LX200 telescope. Fareast uses a 16-inch Meade mounted on an Astelco NTM500 mount with both telescopes using a Quantum Scientific Imaging Charge-coupled device (QSI CCD). Observations were made in the clear band.

Once images of our asteroids had been captured, the images were analysed and the Right-Ascension (RA) and Declination (Dec.) of each object were measured. This was done using an astrometry solution found by matching the observed star field to the expected star field using a relevant star catalogue that would be chosen from our astrometry comparison.

Astrometry Comparison

There are various star catalogues that can be used to apply an astrometric fit to our images. The United States Naval Observatory (USNO) has released several star catalogues and revisions including both the UCAC2 catalogue, released in July 2003, and the UCAC4 catalogue, released in August 2012.[13][14] The USNO catalogues are the most widely used catalogues, however there exist other all-sky catalogues available for use. This includes the Gaia catalogue which is formed from the first data release of the *Gaia* mission with the full catalogue aimed for released in 2022.[15]

These catalogues were chosen for comparison for the following reasons: UCAC2 was the default astrometric solution on the images we were using, UCAC4 was the most recent USNO catalogue released, GAIA was more recent that UCAC4 however it is less complete currently.

The catalogues were compared by taking a sample of our observations of the asteroid Anchises, running the astrometry for each star catalogue and recording the observed RA and Dec. with each star catalogue. These were then compared to the RA and Dec. calculated by JPL's HORIZONS system which produces highly accurate ephemerides that we use as a known control.[16] The results of this comparison are shown in Fig. 3 and Table I.

These results were (in Fig. 3 and Table I) were obtained from 12 observations of Anchises taken on the 24th January 2018 and are reported with 1σ root mean square error. These results show there is a systematic offset in the astrometry solution for UCAC2, specifically Dec, compared to the ephemeris calculated by JPL HORIZONS. UCAC4

and GAIA are both within error of $\Delta Dec = 0$ but have a larger spread than UCAC2. All three star catalogues are within error of $\Delta RA \cos(Dec) = 0$.

These results show that UCAC4 and GAIA are more accurate catalogues than UCAC2, this was expected as UCAC2 is significantly older than the other catalogues. As the star field changes over time, frequent revisions to star catalogues are required to ensure they are viable for accurate observations. Using an older catalogue can introduce greater errors in observations. The difference between UCAC4 and GAIA is indistinguishable with the data set we have used. To further explore their difference and more accurately calculate the systematic offset in these star catalogues, additional observations would be required.

In this work, initially the UCAC2 star catalogue was used in our images. However, based on the results of this preliminary investigation, we took the decision to use astrometry based on the UCAC4 star catalogue as it is accurate to JPL HORIZONS within error. The decision to not use GAIA was based on the catalogue not having a full release published as yet.
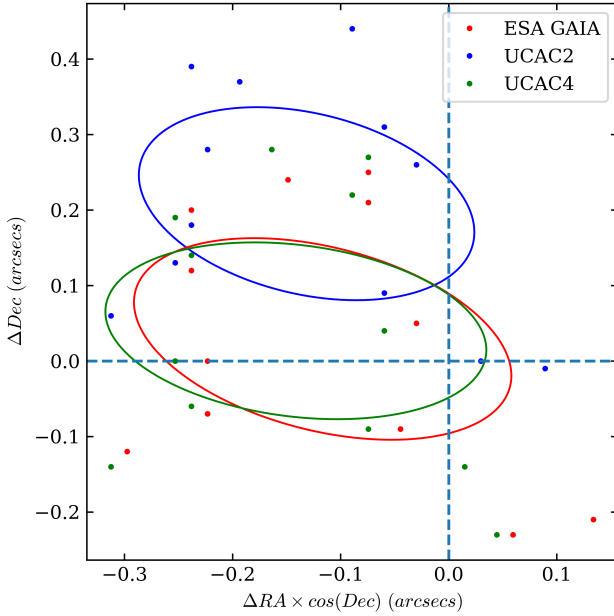

FIG. 3: The difference in $Dec.$ and $RA \cos(Dec)$ between the JPL HORIZONS ephemeris and a sample of 12 observations of Anchises using astrometry solutions from the UCAC2 (blue), UCAC4 (green) and GAIA (red) star catalogues. The 1σ error ellipse is shown for all catalogues. The zero point of both axes is shown as a dashed line, for reference.

dotted Catalogue	Mean $\Delta RA \cos(Dec)$ (arcsecs)	Mean ΔDec (arcsecs)
UCAC2	-0.1 ± 0.1	0.2 ± 0.1
UCAC4	-0.1 ± 0.1	0.0 ± 0.2
GAIA	-0.1 ± 0.1	0.0 ± 0.2

TABLE I: The mean $\Delta RA \cos(Dec)$ and mean ΔDec for the UCAC2, UCAC4 and GAIA star catalogues compared to the JPL HORIZONS epehermis for twelve observations of Anchises. The errors displayed displayed are the 1σ root mean square (RMS) error.

Orbit Determination

To determine the orbits of each asteroid, their RAs and Decs. were measured using the astrometric solution from the UCAC4 catalogue. We then used our results with the Gauss method of determining orbits to calculate their orbital parameters.

The Gauss method is described in detail by Gronchi (2004) and is expanded on by Mitorabi (2014) who details how it can be adjusted from using only 3 observations to using N observations. This is more appropriate for our investigation as we are able to take numerous observations over a period of 7 weeks which should improve the accuracy of our results. An outline of the algorithm for three observations described in "Orbital Mechanics for Engineering Students"[17] is given below:

The orbital parameters can be calculated from the Right Ascension, α_i, and Declination, δ_i, of three observations and also using the observer's position, $\mathbf{R}_i$, at the times of these observations and the times, t_i, of these observations where $i = 1, 2, 3$ corresponds to each distinct observation. This algorithm begins by using the slant range unit vector, defined as $\hat{\mathbf{Q}}_i = \cos\delta_i \cos\alpha_i \hat{\mathbf{I}} + \cos\delta_i \sin\alpha_i \hat{\mathbf{J}} + \sin\delta_i \hat{\mathbf{K}}$ where $\hat{\mathbf{I}}, \hat{\mathbf{J}}, \hat{\mathbf{K}}$ are the heliocentric unit vectors. The algorithm then proceeds as:

1. Calculate the time intervals between observations using the following:

$$\tau_1 = t_1 - t_2, \quad \tau_3 = t_3 - t_2, \quad \tau = \tau_3 - \tau_1. \quad (1)$$

2. Calculate the cross products:

$$\mathbf{p}_1 = \hat{\mathbf{Q}}_2 \times \hat{\mathbf{Q}}_3, \quad \mathbf{p}_2 = \hat{\mathbf{Q}}_1 \times \hat{\mathbf{Q}}_3, \quad \mathbf{p}_3 = \hat{\mathbf{Q}}_1 \times \hat{\mathbf{Q}}_2. \quad (2)$$

3. Calculate $D_0 = \hat{\mathbf{Q}}_1 \cdot \mathbf{p}_1$.

4. Calculate the 9 scalar quantities D_{ij}, $i, j = 1, 2, 3$ where D_{ij} is defined by:

$$D_{ij} = \mathbf{R}_i \cdot \mathbf{p}_j. \quad (3)$$

5. Calculate the quantities A and B given by:

$$A = \frac{1}{D_0}\left(-D_{12}\frac{\tau_3}{\tau} + D_{22} + D_{32}\frac{\tau_1}{\tau}\right), \quad (4)$$

$$B = \frac{1}{6D_0}\left(D_{12}(\tau_3^2 - \tau^2)\frac{\tau_3}{\tau} + D_{32}(\tau^2 - \tau_1^2)\frac{\tau_1}{\tau}\right). \quad (5)$$

6. Calculate the quantity, $E = \mathbf{R}_2 \cdot \hat{\mathbf{Q}}_2$.

7. Calculate the quantities a, b, c using $R_2^2 = \mathbf{R}_2 \cdot \mathbf{R}_2$, $\mu = GM$ where G is Newton's universal gravitational constant and M is the mass of the body being orbited, and the equations:

$$a = -(A^2 + 2AE + R_2^2), \quad (6)$$

$$b = -2\mu B(A + E), \quad (7)$$

$$c = -\mu^2 B^2. \quad (8)$$

8. Find the roots of the equation:

$$x^8 + ax^6 + bx^3 + c = 0, \qquad (9)$$

with the most physically reasonable root equalling r_2. If more than one root seems appropriate, store them and continue the algorithm on all viable roots in parallel and then compare the calculated orbital parameters to the literature.

9. Calculate $Q_2 = A + \mu B / r_2^3$ and Q_1 and Q_3 using the following:

$$Q_1 = \left(\frac{6 \left(D_{31} \frac{\tau_1}{\tau_3} + D_{21} \frac{\tau}{\tau_3} \right) r_2^3 + \mu D_{31} (\tau^2 - \tau_1^2) \frac{\tau_1}{\tau_3}}{6 r_2^3 + \mu (\tau^2 - \tau_3^2)} \right.$$
$$\left. - D_{11} \right) \frac{1}{D_0}, \quad (10)$$

$$Q_3 = \left(\frac{6 \left(D_{13} \frac{\tau_3}{\tau_1} - D_{23} \frac{\tau}{\tau_1} \right) r_2^3 + \mu D_{13} (\tau^2 - \tau_3^2) \frac{\tau_3}{\tau_3 1}}{6 r_2^3 + \mu (\tau^2 - \tau_3^2)} \right.$$
$$\left. - D_{33} \right) \frac{1}{D_0}. \quad (11)$$

10. Calculate the $\mathbf{r}_i$, $i = 1, 2, 3$ vectors using:

$$\mathbf{r_i} = \mathbf{R_i} + Q_i \hat{\mathbf{Q}}_i, \qquad (12)$$

where $\mathbf{r}_i$ $i = 1, 2, 3$ are the position vectors for the object at the time of the three observations used used in this algorithm.

11. Calculate f_i, g_i, $i = 1, 3$ using the equations:

$$f_i \approx 1 - \frac{1}{2} \frac{\mu}{r_2^3} \tau_i^2, \qquad (13)$$

$$g_i \approx \tau_i - \frac{1}{6} \frac{\mu}{r_2^3} \tau_i^3. \qquad (14)$$

12. Calculate $\mathbf{v}_2$ using the equation:

$$\mathbf{v_2} = \frac{1}{f_1 g_3 - f_3 g_1} (-f_3 \mathbf{r_1} + f_1 \mathbf{r_3}), \qquad (15)$$

where $\mathbf{v}_2$ is the velocity vector at the time of the second observation.

13. Calculate the specific angular momentum, $\mathbf{h}$:

$$\mathbf{h} = \mathbf{r_2} \times \mathbf{v_2}. \qquad (16)$$

14. Calculate the inclination using the z-component of $\mathbf{h}$, h_z:

$$i = \arccos \left(\frac{h_z}{|\mathbf{h}|} \right). \qquad (17)$$

15. Calculate the vector that defines the node line, N, using:

$$\mathbf{N} = \hat{\mathbf{K}} \times \mathbf{h}. \qquad (18)$$

16. Calculate the RA of the ascending node:

$$\Omega = \arccos \left(\frac{N_x}{|\mathbf{N}|} \right), \qquad (19)$$

where N_x is the x component of $\mathbf{N}$.

17. Calculate the eccentricity vector, $\mathbf{e}$, using:

$$\mathbf{e} = \frac{1}{\mu} \left[\left(\mathbf{v}^2 - \frac{\mu}{|\mathbf{r}|} \right) \mathbf{r} - (\mathbf{r} \cdot \mathbf{v}) \mathbf{v} \right], \qquad (20)$$

where the eccentricity orbital parameter, e, is given by $e = |\mathbf{e}|$.

18. Calculate the argument of perigee, ω, using:

$$\omega = \arccos \left(\frac{\mathbf{N} \cdot \mathbf{e}}{|\mathbf{N}||\mathbf{e}|} \right). \qquad (21)$$

19. Calculate the true anomaly, ν, using:

$$\nu = \arccos \left(\frac{\mathbf{e} \cdot \mathbf{r}}{|\mathbf{e}||\mathbf{r}|} \right). \qquad (22)$$

From the parameters $\mathbf{h}$, i, Ω, ω, e, ν, all other orbital parameters can be derived.

The implementation of the Gauss method we use is the Find_Orb Orbit determination software.[18] To verify that this returns accurate results, we use RA and Decs. from an ephemeris generated by JPL HORIZONS and investigate if the calculated orbital parameters from Find_Orb converge to the JPL result. We would expect this to happen if the software was functioning correctly.

This analysis was first performed using an ephemeris of Patroclus for one observation per week for 13 weeks. This is approximately equal to the number of observations we took in this investigation over the same time frame. The results of this preliminary investigation are shown in Fig. 4.

These results show that, generally, Find_Orb's solutions do converge to the JPL HORIZONS orbital parameters. However, the results are very noisy showing a large variance in the solutions being returned. This is most likely due to the observations being taken from a small arc of the orbit.

To investigate the effect of a greater arc of observations and to see if this improves convergence, this investigation was performed again. However, the observations were taken from the JPL HORIZONS ephemeris for one observation per month for 18 months and excluding those that would be below the horizon in Durham.

Fig. 5 shows that the convergence to the literature values is greater and faster when using observations taken from a greater arc length of the orbit, as in this case all parameters reach a a fractional residual $< 10^{-5}$ after 8 observations; this does not happen for the shorter arc of observations. These results show that using observations covering a longer time frame produce more accurate results. Therefore, in this investigation we couple our own observations with archival data. Both Fig. 4 and Fig. 5 show that a good level of convergence can be found using the Find_Orb software and this implementation would be suitable for this investigation.

We proceeded with using Find_Orb to determine the orbital parameters of our asteroids. To supplement our observations of Patroclus and Priamus, archival data was acquired. For Patroclus, 9 further observations from 2001 to
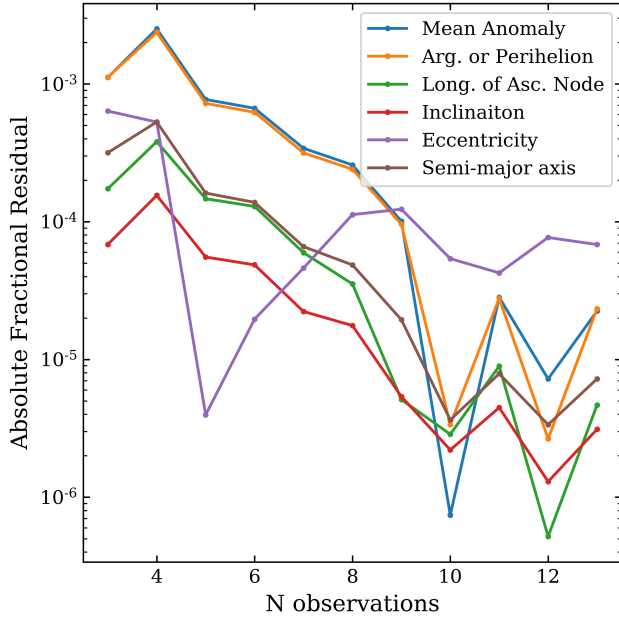
FIG. 4: The absolute fractional residual between the Find_Orb orbital parameters and the JPL HORIZONS parameters using an increasing number of ephemeris observation points over 13 weeks.
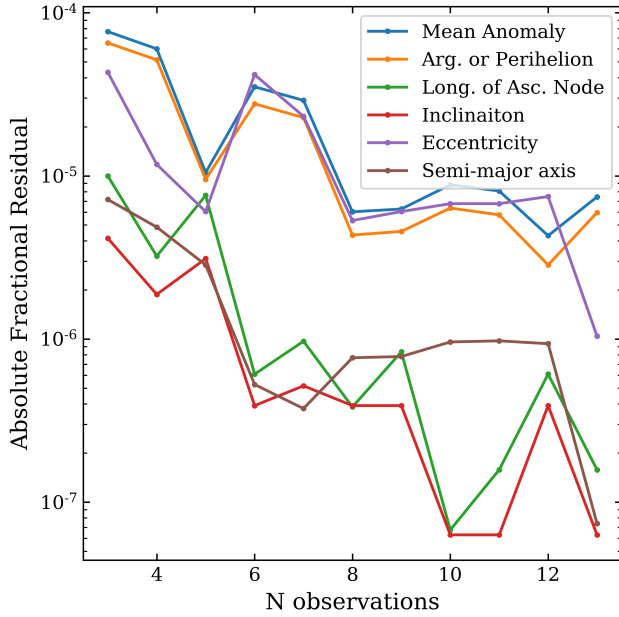

FIG. 5: The absolute fractional residual between the Find_Orb calculated orbital parameters and the JPL HORIZONS parameters using an increasing number of ephemeris observation points over 18 months.

2017 and for Priamus, 5 further observations from 2011 to 2016 were acquired and used to improve the accuracy and error confidence in the calculated orbital parameters.

The errors on the orbital parameters were calculated using a jackknifing method: assuming we have N observations, we systematically remove one observation from the data set, we then calculate and keep a record of the orbital parameters on this set of $N - 1$ observations. This is repeated until every observation has been removed once. We then have a distribution for each orbital parameter that is fit

to a gaussian where the mean is the orbital parameter of the population and the standard deviation is the error on that parameter. In this investigation, all quoted errors represent the 1σ uncertainty unless otherwise stated.

Positional Prediction

Once the orbital parameters had been acquired, they were used to predict the position of the asteroid at any given time. This is not trivial as it must take account of the osculating orbit, as previously discussed.

We used the Pyephem python package with the calculated orbital parameters and epochs to determine the position of the asteroid at a given time. The specific algorithms are described in detail by Peter Duffett-Smith and Jonathan Zwart in "Practical Astronomy with your Calculator or Spreadsheet."[19, p.121-130] An outline of the method to calculate the heliocentric position is given here:

The heliocentric Cartesian coordinates, x, y, z, can calculated from a body's Keplerian orbital parameters.

1. Numerically solve the following equation for the eccentric anomaly, E, from the mean anomaly, M, and eccentricity, e:

$$M = E - e\sin E. \qquad (23)$$

2. Calculate the true anomaly, ν, from the eccentric anomaly and eccentricity using the equation:

$$\tan\frac{\nu}{2} = \left(\frac{1+e}{1-e}\right)^{1/2}\tan\frac{E}{2}. \qquad (24)$$

3. Calculate the radial distance, r, from the semi-major axis, a, using the equation:

$$r = a(1 - e\cos E). \qquad (25)$$

4. Calculate the x, y, z coordinates using the equations:

$$x = r(\cos\Omega\cos(\omega+\nu) - \sin\Omega\sin(\omega+\nu)\cos i), \quad (26)$$

$$y = r(\sin\Omega\cos(\omega+\nu) + \cos\Omega\sin(\omega+\nu)\cos i), \quad (27)$$

$$z = r\sin i\sin(\omega+\nu). \qquad (28)$$

Equations (26), (27) and (28) define the heliocentric coordinate position of the asteroid with the x-axis direction based on the epoch of the mean anomaly and in the plane of the ecliptic, the y-axis perpendicular to the x axis in the plane of the ecliptic and the z-axis normal to the ecliptic.

The errors on the orbital parameters are propagated through to the calculated position by generating a sample of orbital parameters that are perturbed by a random Gaussian distribution with the mean as the orbital parameter and standard deviation equal to the error on the orbital parameter. Positions can then be calculated from this randomised sample, producing a distribution of positions for the asteroid. The error in each Cartesian direction is then given by the square root of the diagonal elements of the covariance matrix of this position distribution. We generate an error

ellipsoid from this distribution using the eigenvalues and eigenvectors of the covariance matrix where the roots of the eigenvalues give the error in each direction of the basis defined by the eigenvectors. The roots of the eigenvalues are used as the principal semi-axes of the ellipsoid. The volume of the ellipsoid gives the confidence volume, the volume of an ellipsoid, V, is given by:

$$V = \frac{4}{3}\pi abc, \tag{29}$$

where a, b, c are the principal semi-axes lengths and are equal to the root of the eigenvalues of the covariance matrix.

Orbital Transfer

Once the position of the asteroid has been determined, the possible orbital transfers to the asteroid can be investigated. For this investigation we assume that the *Lucy* spacecraft will perform a Hohmann transfer from a parking orbit at the Earth's heliocentric radius to the asteroid's predicted position, within the plane of the asteroid's orbit.

A Hohmann transfer assumes an initial circular parking orbit in the plane of the target orbit. It consists of two instantaneous burns. The first takes the initial circular orbit to an elliptical orbit with its apoapsis at the radius of the target orbit. The second burn then occurs at the apoapsis of the elliptical orbit to convert the elliptical orbit to the target orbit. Fig. 6 shows an illustration of the Hohmann transfer orbit, where Δv_1 and Δv_2 represent the first and second burns respectively.
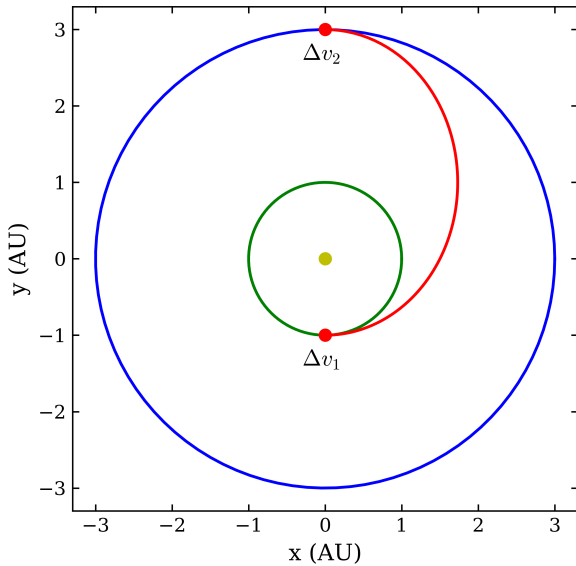

FIG. 6: The green and blue lines represent circular orbits around the Sun (yellow point) with radii equal to 1 and 3 AU respectively. The red line represents the Hohmann transfer. The burn positions are marked with red points and text. The Δv requirement of each burn are given in Equations (30) and (31).

The change in velocity required to achieve these orbits is given by the following equations:

$$\Delta v_1 = \sqrt{\frac{\mu}{r_1}} \left(\sqrt{\frac{2r_2}{r_1 + r_2}} - 1 \right), \tag{30}$$

$$\Delta v_2 = \sqrt{\frac{\mu}{r_2}} \left(1 - \sqrt{\frac{2r_1}{r_1 + r_2}} \right), \tag{31}$$

where r_1 is the radius of the inner orbit, r_2 is the radius of the outer orbit and $\mu = GM$ where G is Newton's gravitational constant and M is the mass of the body being orbited, in our case the Sun. The total velocity change required by the Hohmann transfer, Δv_T is given trivially by the sum of Δv_1 and Δv_2.

Using our calculated positions for Patroclus, we find the maximum and minimum radii of the 1σ error ellipsoid. We then use Equations (30) and (31) to calculate the range in Δv_T due to the uncertainty in Patroclus' calculated position. For the *Lucy* mission, we place an upper bound on the Δv_T requirement in order to reduce the fuel requirement and hence the mass of the spacecraft.

Modelling the orbital transfer to Patroclus as a Hohmann transfer from a parking orbit at Earth's radius is a simplification to the flight plan originally suggested for the *Lucy* mission which will first fly to the L4 camp of Trojan asteroids before switching to Patroclus in the L5 camp using a complex set of orbital manoeuvres.[20] However, this simplified orbital transfer will highlight the difference in Δv requirements from increasing the confidence in the calculated position for Patroclus.

III. RESULTS

The observations acquired in this investigation from 24th January 2018 to 10th March 2018 are shown in Fig. 7.
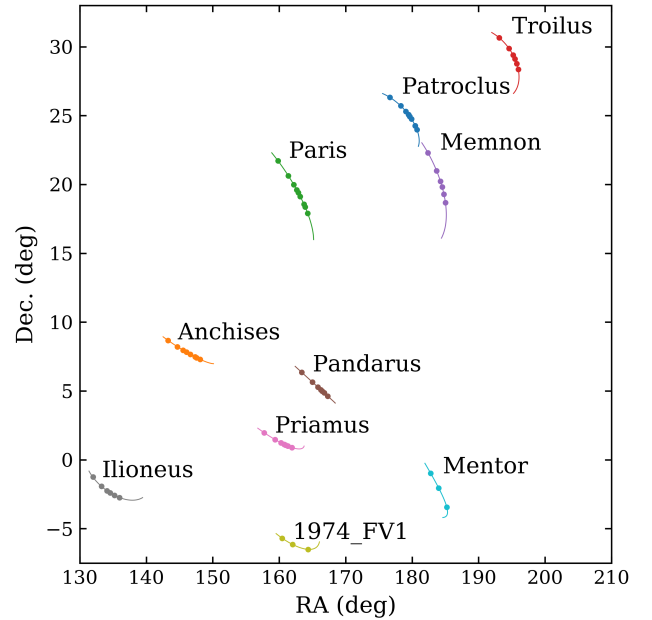
FIG. 7: Right-Ascensions and Declinations of asteroids acquired during our observations. Solid lines represent the expected movement of the asteroids during the 7 week observing period. The orbital parameters used were obtained from the IAU Minor Planet Centre.[21]

The Find_Orb software was used to fit orbits to eight of our ten asteroids. 1974 FV1 and Mentor could not be fitted to orbits as only 3 observations for each were attained. The jackknifing technique used to obtain errors on the orbital

FIG. 8: The absolute fractional residual between our calculated orbital parameters and the literature as the number of observations increases for Patroclus.

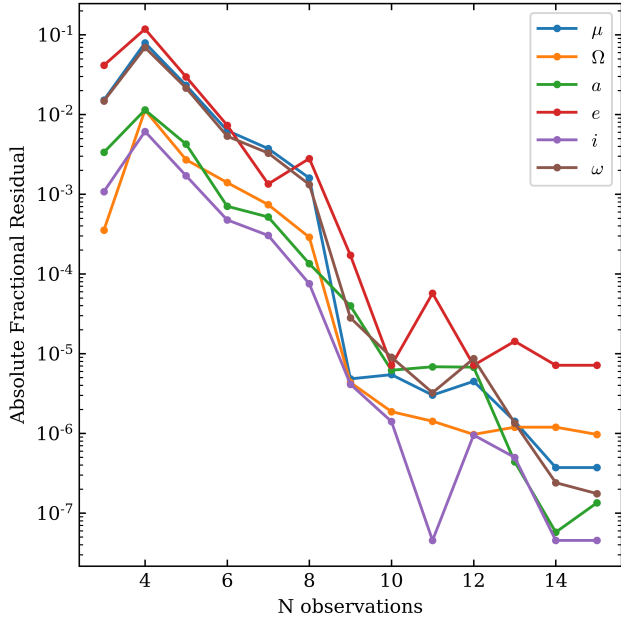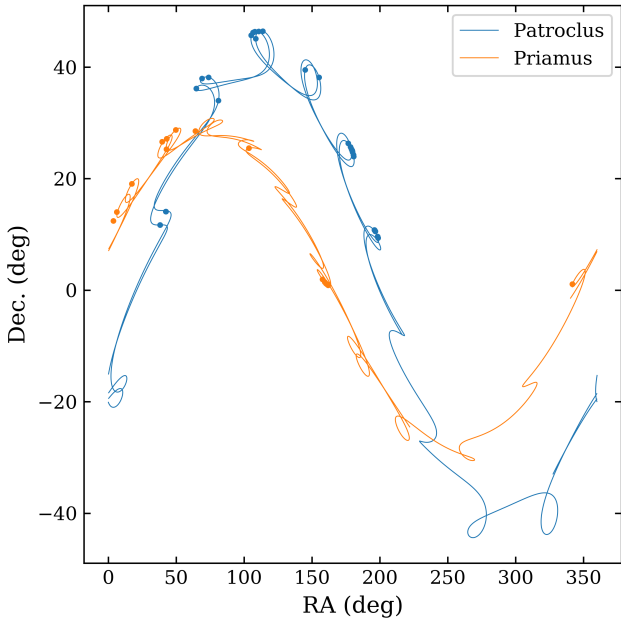FIG. 9: The points represent the observations used to calculate their orbital parameters in Table V. The line represents its literature orbital path from the 1st January 2000 to the 1st January 2020. There are two distinct lines for each asteroid as the orbital period is ∼12 years and so each asteroid will complete ∼1.7 orbits.

parameters requires at least 4 observations. The orbital parameters are given in Table IV.

This demonstrates that the method used in this investigation is suitable for acquiring orbital parameters, as all parameters for 3 asteroids were found to match within 1σ error of the literature, and a further 4 asteroid's parameters found to within 3σ error of the literature. Ilioneus was the only asteroid that did not fall in either of these two groups which is most likely due to a lack of observations as it was only
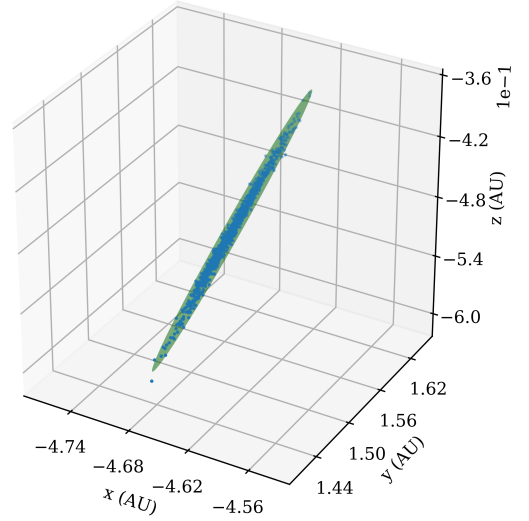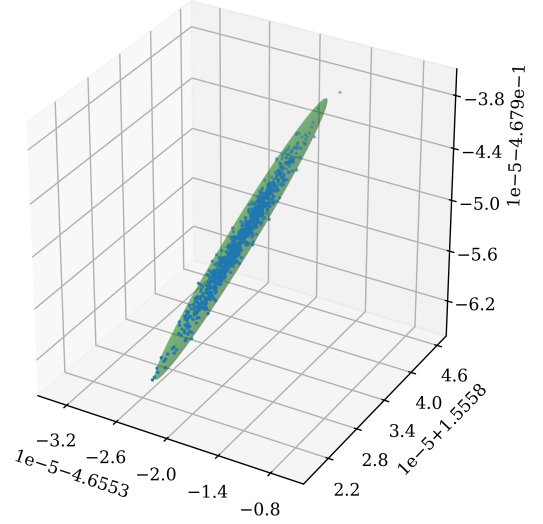

FIG. 10: The distribution of positions for Patroclus calculated from its orbital parameters including (top panel) and excluding (bottom panel) archival data. The error ellipsoid shown is at the 3σ confidence level.

observed on 4 nights. Table IV shows smaller errors were achievable with more observations. This is supported by Fig. 8 that shows that as the number of observations used in the orbit solution is increased, the results better converge to the literature value.

Our own observations can also be combined with archival data for Patroclus and Priamus to improve the accuracy of the calculated orbital parameters. The archival observations used are displayed in Fig. 9 and the improved orbital parameters are displayed in Table V.

Both sets of orbital parameters for Patroclus (from Table IV and Table V) were used to calculate its predicted position for the date of 2nd March 2033, this being the planned date for *Lucy* to flyby Patroclus. The results of the predicted position are given in Table II with error ellipsoids for their positions given in Fig. 10. The ellipsoids shown in Fig. 10 provide the 3σ uncertainty in the asteroids position.

These calculated positions can be used to place an upper and lower bound on the Δv_T requirement for a Hohmann

	x (AU)	y (AU)	z (AU)
Excluding archival data	-4.655 ± 0.006	1.53 ± 0.04	-0.49 ± 0.03
Including archival data	-4.6553203 ± 0.0000009	1.555832 ± 0.000004	-0.467951 ± 0.000003
Literature	-4.6553217	1.555834	-0.467952

TABLE II: The position of Patroclus on 2nd March 2033, the date of the *Lucy* mission rendezvous. The uncertainties given are for a 1σ confidence region. The literature values given were calculated using the orbital parameters from JPL HORIZONS.

	Upper bound, $\Delta v_{T,u}$ (km s^{-1})	Lower bound, $\Delta v_{T,l}$ (km s^{-1})	$\frac{2(\Delta v_{T,u} - \Delta v_{T,l})}{\Delta v_{T,u} + \Delta v_{T,l}}$
Excluding archival data	14.243	14.236	4.9×10^{-4}
Including archival data	14.243685	14.243684	7.0×10^{-8}

TABLE III: The upper and lower bounds for a Hohmann transfer to the positions in Table II based on their errors. The fractional difference in the bounds is also displayed.

transfer in the plane of the orbit of the asteroid. These upper and lower bounds are given in Table III. The inclusion of archival data can significantly improve the range of the bounds, the fractional difference decreasing by four orders of magnitude from 4.9×10^{-4} to 7.0×10^{-8}.

IV. DISCUSSION

A preliminary investigation was performed to determine the accuracies of various star catalogues. For UCAC2, this found a systematic error of 0.2 ± 0.1 arcsecs in Dec. compared to the JPL HORZONS ephemeris. Initially, this was the star catalogue being used in our images, however, based on this result we took the decision to use astrometry based on the UCAC4 star catalogue as this was accurate to JPL HORIZONS within error. The decision to not use GAIA was based on that catalogue not having a full release published as yet.

Our initial sample choice of asteroids provided good observations, with two asteroids, 1974 FV1 and Mentor, not producing enough observations to perform orbit determination. The low height of these asteroids in the sky resulted in observations not being possible on some nights where the rest of our asteroid sample was visible. Orbit determination was then run using the Find_Orb software with all parameters for 3 asteroids within 1σ errors of the literature and all parameters for a further 4 asteroids within 3σ errors of the literature. The literature values were taken from JPL HORIZONS. The main reason that only 3 asteroids were within 1σ errors is that our observations only ranged from the 24th January to the 10th March, a span of 45 days. As the approximate time period of a circular Trojan orbit is 12 years (4380 days), using our own observations we only covered an arc length of $\sim 1\%$ of its total orbit which produces more inaccurate results with larger errors compared to a longer arc length.

It is shown trivially in Figures 4 and 5 that, generally, as the number of observations increases the orbital parameters better converge to the literature values. Fig. 5 shows

that increasing the time step between observations can produce more accurate results. This supports the notion that more accurate results can be achieved by maximising the observed arc length of its orbit.

We sourced archival data for Patroclus and Priamus to supplement our own observations, the orbital parameters were then recalculated. Using this archival data, the arc length of observations was significantly increased: for Patroclus, the earliest data obtained was from October 2001 and so we had sufficient data to cover ~ 1.4 orbits; for Priamus, data was obtained from October 2011 and so we had archival data covering $\sim 50\%$ of its total orbit.

These greater arc lengths allowed a solution with a far greater confidence to be calculated from our bootstrapping method. The mean fractional uncertainty in our orbital parameters for Patroclus using only our own observations is 8.1×10^{-4}. This reduces by 3 orders of magnitude to 3.5×10^{-7} when the archival data is included in the computation of the orbital parameters. We find similar improvements for Priamus which has a mean fractional uncertainty of 3.8×10^{-3} using our own observations which reduces to 2.4×10^{-6} including archival data. These results highlight the importance of supplementing our own observations with archival data allowing our 1σ confidence regions to be significantly reduced. This is important to the aim of this investigation as these errors are propagated through to the calculation of Patroclus' position for the *Lucy* rendezvous.

The orbital parameters calculated using archival data have significantly smaller error bars associated with them than compared to those calculated using only our own observations. Only 2 parameters are within 1σ error bars of the literature however if the error bars are extended to 3σ, a further 7 are in agreement. The small differences between our values and the literature may not be due to errors in our method. These asteroids have osculating orbital parameters, meaning that they change over time. The JPL HORIZONS orbital parameters for Patroclus were calculated on 21st June 2017, whereas our orbital parameters use an epoch of osculation based on the mean date of our observations. As these parameters change over time, significant differences in epochs such as this are likely to be the cause of our results not aligning exactly with the literature.

Using our calculated orbital parameters for the prediction of Patroclus' position, we calculated the 1σ error ellipsoid based on the distribution of possible positions. The error ellipsoid has semi-major axis lengths equal to the eigenvalues of the covariance matrix of the position distribution. The volume of the 1σ ellipsoid calculated solely from our own observations is 1.7×10^{-7} AU^3, whereas the volume of the ellipsoid found using orbital parameters including the archival data is 3.6×10^{-18} AU^3. This is a significant improvement in confidence region with the volume decreasing by a factor of $\sim 10^{11}$.

This could make a highly significant difference to a NASA mission such as *Lucy* which has very limited constraints on resources such as fuel. To investigate the effect of this on the fuel requirements, the maximum radii from the error ellipsoids including and excluding archival data were used to find Δv requirements of a Hohmann transfer to the positions calculated for Patroclus. The calculated bounds on the Δv_T requirements are given in Table III. These show that the difference in the bounds on the Δv_T requirement can be significantly reduced if using a position of Patroclus with smaller error bars with the uncertainty

Asteroid		Mean Anomaly, M (°)	Argument of Perihelion, ω (°)	Longitude of Ascending Node, Ω (°)	Semi-major axis, a (AU)	Eccentricity, e	Inclination, i (°)	Number of Observations
Anchises	Observed	294 ± 2	39 ± 2	284.2 ± 0.2	5.29 ± 0.02	0.147 ± 0.006	6.96 ± 0.03	7
	Literature	294	41	283.9	5.31	0.139	6.91	
Ilioneus	Observed	221 ± 5	220 ± 10	242.0 ± 0.2	5.6 ± 0.1	0.13 ± 0.03	15.48 ± 0.08	4
	Literature	320	112	242.5	5.23	0.01	15.7	
Memnon	Observed	334 ± 2	277 ± 2	133.94 ± 0.07	5.239 ± 0.002	0.052 ± 0.001	27.20 ± 0.04	5
	Literature	336	275	133.98	5.236	0.051	27.22	
Pandarus	Observed	92 ± 1	41 ± 1	179.78 ± 0.01	5.182 ± 0.002	0.068 ± 0.001	1.856 ± 0.002	7
	Literature	92	40	179.79	5.183	0.068	1.854	
Paris	Observed	65.40 ± 0.07	150.61 ± 0.04	135.909 ± 0.005	5.2221 ± 0.0001	0.1270 ± 0.0003	27.852 ± 0.006	9
	Literature	65.61	150.49	135.918	5.2222	0.1278	27.863	
Patroclus	Observed	324.8 ± 0.4	308.2 ± 0.3	44.38 ± 0.01	5.220 ± 0.001	0.1398 ± 0.0003	22.049 ± 0.002	9
	Literature	325.2	307.9	44.37	5.218	0.1400	22.053	
Priamus	Observed	44.9 ± 0.2	335.1 ± 0.1	301.60 ± 0.05	5.173 ± 0.002	0.123 ± 0.002	8.912 ± 0.009	7
	Literature	44.8	335.2	301.64	5.172	0.124	8.919	
Troilus	Observed	247 ± 2	295 ± 2	48.56 ± 0.03	5.241 ± 0.003	0.0912 ± 0.0005	33.56 ± 0.01	6
	Literature	247	295	48.56	5.240	0.0911	33.56	

TABLE IV: The calculated orbital parameters for 8 of our observed asteroids. The number of observations used to calculate the parameters is also given in the right-most column. The literature values were taken from JPL HORIZONS.[16] The epochs of the literature and observed results were the same.

Asteroid		Mean Anomaly, M (°)	Argument of Perihelion, ω (°)	Longitude of Ascending Node, Ω (°)	Semi-major axis, a (AU)	Eccentricity, e	Inclination, i (°)	Number of Observations
Patroclus	Observed	325.19538 ± 0.00004	307.85954 ± 0.00003	44.365937 ± 0.000009	5.2184995 ± 0.0000001	0.1399506 ± 0.0000002	22.052693 ± 0.000005	17
	Literature	325.19545	307.85953	44.365963	5.2184997	0.1399500	22.052699	
Priamus	Observed	44.7601 ± 0.0002	335.2247 ± 0.0002	301.63926 ± 0.00008	5.171862 ± 0.000004	0.1237472 ± 0.0000009	8.91919 ± 0.00001	17
	Literature	44.7607	335.2235	301.63945	5.171847	0.1237506	8.91919	

TABLE V: The calculated orbital parameters for 2 of our observed asteroids including the archival data. The number of observations used to calculate the parameters is also given in the right-most column.

in the Δv_T requirement being reduced from 4.9×10^{-4} to 7.0×10^{-8} with the inclusion of the archival data.

This reduction in the uncertainty of the Δv_T requirement would be beneficial for the *Lucy* mission as a high level of accuracy is required when performing orbital manoeuvres and performing a flyby with the lowest possible separation with Patroclus. Highly accurate positions are required for rendezvous manoeuvres with minor planets to achieve an optimal flyby. However, this reduction in Δv_T uncertainty would not be significantly beneficial in reducing the mass of the *Lucy* mission as a fractional uncertainty of 4.9×10^{-4} equates to $\Delta v \approx 7 \text{ m s}^{-1}$, an amount largely negligible when considering $\Delta v_T \approx 14 \text{ km s}^{-1}$ for the complete Hohmann transfer and hence the mass of fuel this would equate to would also be negligible.

V. CONCLUSIONS

Our investigation aimed to accurately determine the position of Patroclus for the *Lucy* mission flyby. We did this by initially selecting 10 asteroids to study. Observations of

these were taken using the Far-East 16, DRACO2 and Pt5m telescopes in the clear band over a period of 7 weeks. Before positional measurements could be taken from our images, the varying star catalogues were investigated.

The UCAC2, UCAC4 and GAIA star catalogues were compared to investigate their deviations from the JPL HORIZONS ephemeris calculator. UCAC4 and Gaia were found to be in agreement with JPL HORIZONS within error; however, UCAC2 was found to have a deviation from JPL HORIZONS of 0.2 ± 0.1 in declination. This was not surprising from an older star catalogue. Using these results, the UCAC4 catalogue was selected for use in this investigation.

Once the positions of our asteroids in terms of RA and Dec. were measured from our images, we used an implementation of the Gauss method to determine their orbital parameters. This implementation was verified and found to converge to the orbital parameters given by JPL HORIZONS. The orbital parameters were determined for 80% of our initial asteroid sample; however, orbital parameters could not be determined for 1974 FV1 and Mentor as an insufficient number of observations were taken. Archival data

was obtained for Patroclus and Priamus and supplemented with our own observations to determine improved orbital parameters for these asteroids.

All orbital parameters calculated using solely our own observations for 7 of our asteroids were found to be consistent with the literature within 3σ error bars. The main cause of inaccuracies is most likely the short arc of observation we had of our asteroids; our observations only covered $\sim 1\%$ of the asteroid's full orbit. With the improved orbital parameters for Patroclus and Priamus, 9 of the 12 orbital parameters are in agreement with JPL HORIZONS. Inaccuracies in this case were most likely due to a difference in the epoch of osculation for our parameters, with our epoch being taken as the average day of observation. This differed to JPL HORIZONS which depended on when the calculation was performed. In the case of Patroclus, this was 21st June 2017.

We then used the orbital parameters for Patroclus to calculate its predicted position for the *Lucy* mission rendezvous. The positions using orbital parameters including and excluding archival data were calculated. The confidence in the position including archival data was significantly higher than the position calculated excluding the archival data, the volume of the 1σ error ellipsoid reducing by a factor of $\sim 10^{11}$.

An upper and lower bound of Δv requirement for a Hohmann transfer was then calculated. The fractional uncertainty in the Δv requirement could be reduced from 4.9×10^{-4} to 7.0×10^{-8}. This is significant for performing an accurate orbital transfer as high level of accuracy is required when performing the manoeuvre. When considering fuel requirements for the Hohmann transfer, a fractional uncertainty of 4.9×10^{-4} equates to $\Delta v \approx 7\,\mathrm{m\,s^{-1}}$. This is negligible compared to the $\Delta v \approx 14\,\mathrm{km\,s^{-1}}$ of the complete Hohmann transfer.

References

[1] "List Of Jupiter Trojans." https://www.minorplanetcenter.net/iau/lists/JupiterTrojans.html.

[2] H. J. Fleming and D. P. Hamilton, "On the origin of the Trojan asteroids: Effects of Jupiter's mass accretion and radial migration," *Icarus*, vol. 148, pp. 479–493, Dec. 2000.

[3] E. M. Shoemaker, C. S. Shoemaker, and R. F. Wolfe, "Trojan asteroids - Populations, dynamical structure and origin of the L4 and L5 swarms," pp. 487–523, 1989.

[4] S. J. Kortenkamp and D. P. Hamilton, "Capture of Trojan Asteroids in the Early Solar Nebula," vol. 33, p. 25.06, Nov. 2001.

[5] J. P. Emery, F. Marzari, A. Morbidelli, L. M. French, and T. Grav, "The Complex History of Trojan Asteroids," *arXiv:1506.01658 [astro-ph]*, 2015.

[6] A. Morbidelli, H. F. Levison, K. Tsiganis, and R. Gomes, "Chaotic capture of Jupiter's Trojan asteroids in the early Solar System," *Nature*, vol. 435, pp. 462–465, May 2005.

[7] D. Nesvorný, D. Vokrouhlický, and A. Morbidelli, "Capture of Trojans by Jumping Jupiter," *The Astrophysical Journal*, vol. 768, no. 1, p. 45, 2013.

[8] M. W. Buie, C. B. Olkin, W. J. Merline, K. J. Walsh, H. F. Levison, B. Timerson, D. Herald, W. M. Owen Jr., H. B. Abramson, K. J. Abramson, D. C. Breit, D. B. Caton, S. J. Conard, M. A. Croom, R. W. Dunford, J. A. Dunford, D. W. Dunham, C. K. Ellington, Y. Liu, P. D. Maley, A. M. Olsen, S. Preston, R. Royer, A. E. Scheck, C. Sherrod, L. Sherrod, T. J. Swift, L. W. Taylor III, and R. Venable,

"SIZE AND SHAPE FROM STELLAR OCCULTATION OBSERVATIONS OF THE DOUBLE JUPITER TROJAN PATROCLUS AND MENOETIUS," *The Astronomical Journal*, vol. 149, p. 113, Feb. 2015.

[9] F. Marchis, D. Hestroffer, P. Descamps, J. Berthier, A. H. Bouchez, R. D. Campbell, J. C. Y. Chin, M. A. van Dam, S. K. Hartman, E. M. Johansson, R. E. Lafon, D. Le Mignant, I. de Pater, P. J. Stomski, D. M. Summers, F. Vachier, P. L. Wizinovich, and M. H. Wong, "A low density of 0.8gcm-3 for the Trojan binary asteroid 617Patroclus," *Nature*, vol. 439, pp. 565–567, Feb. 2006.

[10] B. Yang and D. Jewitt, "Spectroscopic Search for Water Ice on Jovian Trojan Asteroids," vol. 38, p. 50.03, Sept. 2006.

[11] "File:Orbit1.svg." https://en.wikipedia.org/wiki/File:Orbit1.svg#filelinks.

[12] "Mean anomaly diagram.png." https://commons.wikimedia.org/wiki/File:Mean_anomaly_diagram.png, Oct. 2015.

[13] N. Zacharias, S. E. Urban, M. I. Zacharias, G. L. Wycoff, D. M. Hall, D. G. Monet, and T. J. Rafferty, "The second US Naval Observatory CCD Astrograph Catalog (UCAC2)," *The Astronomical Journal*, vol. 127, pp. 3043–3059, May 2004.

[14] N. Zacharias, C. Finch, T. Girard, A. Henden, J. Bartlett, D. Monet, and M. Zacharias, "The Fourth US Naval Observatory CCD Astrograph Catalog (UCAC4)," Dec. 2012.

[15] G. Collaboration, A. G. A. Brown, A. Vallenari, T. Prusti, J. de Bruijne, F. Mignard, R. Drimmel, and . co-authors, "Gaia Data Release 1. Summary of the astrometric, photometric, and survey properties," *Astronomy & Astrophysics*, vol. 595, p. A2, Nov. 2016.

[16] "HORIZONS System." https://ssd.jpl.nasa.gov/?horizons.

[17] H. D. Curtis, *Orbital Mechanics for Engineering Students*. Elsevier Aerospace engineering series, Amsterdam: Elsevier/Butterworth-Heinemann, 1. ed., reprinted ed., 2008. OCLC: 552116374.

[18] "Find_Orb Orbit determination software." https://www.projectpluto.com/find_orb.htm.

[19] P. Duffett-Smith, J. Zwart, and P. Duffett-Smith, *Practical Astronomy with Your Calculator or Spreadsheet*. Cambridge ; New York: Cambridge University Press, 4th ed ed., 2011. OCLC: ocn670374857.

[20] "47th Lunar and Planetary Science Conference." https://www.hou.usra.edu/meetings/lpsc2016/.

[21] "IAU Minor Planet Center." https://www.minorplanetcenter.net/iau/mpc.html.

Appendix A: Observing Log

Date (2018)	Telescope	Conditions	Objects Observed
24th January	Far-East 16	Cloudy	Anchises, Paris, Patroclus
29th January	Far-East 16	Cloudy/Clear	Anchises, Paris, Patroclus
31st January	Far-East 16	Cloudy/Clear	1974 FV1, Anchises, Ilioneus, Memnon, Mentor, Pandarus, Paris, Patroclus, Priamus, Troilus
6th February	Far-East 16	Cloudy/Clear	Anchises, Ilioneus, Memnon, Pandarus, Paris, Patroclus, Priamus, Troilus
9th February	DRACO2	Clear	Pandarus, Paris, Patroclus, Priamus
11th February	DRACO2	Clear	Anchises, Ilioneus, Memnon, Pandarus, Paris, Patroclus, Priamus, Troilus
15th February	Far-East 16	Clear	Anchises, Ilioneus, Memnon, Pandarus, Paris, Patroclus, Priamus, Troilus
22nd February	Far-East 16	Cloudy/Clear	1974 FV1, Anchises, Ilioneus, Memnon, Mentor, Pandarus, Paris, Patroclus, Priamus, Troilus
7th March	Far-East 16	Clear	1974 FV1, Anchises, Ilioneus, Memnon, Mentor, Pandarus, Paris, Patroclus, Priamus, Troilus
10th March	Pt5m	Cloudy	Patroclus

TABLE VI: A record of the observations taken during the course of this investigation.

Asteroid	Observations
Patroclus	27th October 2001, 26th January 2003, 1st February 2004 5th February 2007, 17th October 2013, 24th September 2014, 13th January 2015, 13th March 2016, 12th January 2017
Priamus	15th October 2011, 9th October 2012, 29th October 2013, 23rd January 2014, 2nd February 2016

TABLE VII: A record of the observations taken during the course of this investigation.

Table VI gives a detailed observing log of all observations taken during the course of this investigation. Given in Table VII is a record of all archival observations used in this investigation.

Appendix B: Error Ellipses for Patroclus Position

The errors in the position of Patroclus were calculated using the covariance matrix of the distribution of positions. The covariance matrix, $\mathbf{C}$, for the positions is given below:

$$\mathbf{C} = \begin{bmatrix} E_{xx} & E_{xy} & E_{xz} \\ E_{yx} & E_{yy} & E_{yz} \\ E_{zx} & E_{zy} & E_{zz} \end{bmatrix}, \quad \text{(B1)}$$

where $E_{ij} = E[(i - \mu_i)(j - \mu_j)]$, $i, j = X, Y, Z$; E is the expectation operator; X, Y, Z are the corresponding set of Cartesian coordinates; μ_X, μ_Y, μ_Z are the mean of the corresponding Cartesian coordinate set.

The root of the diagonal elements of $\mathbf{C}$, E_{xx}, E_y, E_{zz}, are used as the error in each Cartesian coordinate. Explicitly:

$$\sigma_x = \sqrt{E_{xx}}, \quad \text{(B2)}$$
$$\sigma_y = \sqrt{E_{yy}}, \quad \text{(B3)}$$
$$\sigma_z = \sqrt{E_{zz}}, \quad \text{(B4)}$$

where $\sigma_x, \sigma_y, \sigma_z$ is the error in the respective Cartesian coordinate and these are the errors used in Table II.

The eigenvalues, λ_1, λ_2, λ_3; and eigenvectors, $\mathbf{v}_1$, $\mathbf{v}_2$, $\mathbf{v}_3$; of $\mathbf{C}$ can then be found to construct the error ellipsoid. The roots of the eigenvalues represent the semi-axis lengths of the ellipsoid. The ellipsoid is rotated so that each eigenvalue semi-axis length is aligned in the direction of its corresponding eigenvector.

Appendix C: Computational Programs

All code used to produce the results in this investigation is available here: `https://github.com/baldimort/Trojans-Lucy-Mission`.